

Supplement of

Exploring the regolith with electrical resistivity tomography in large-scale surveys: electrode spacing related issues and possibility

Laurent Gourdol¹, Rémi Clément², Jérôme Juilleret¹, Laurent Pfister¹, Christophe Hissler¹

¹ Catchment and Eco-hydrology Research Group (CAT), Luxembourg Institute of Science and Technology (LIST), Belvaux, L-4422, Luxembourg

² REVERSAAL Research Unit, National Research Institute for Agriculture, Food and Environment (INRAE), Villeurbanne, F-69626, France

Correspondence to: Laurent Gourdol (laurent.gourdol@list.lu)

Contents of this file

Figures S1-S15

Tables S1-S2

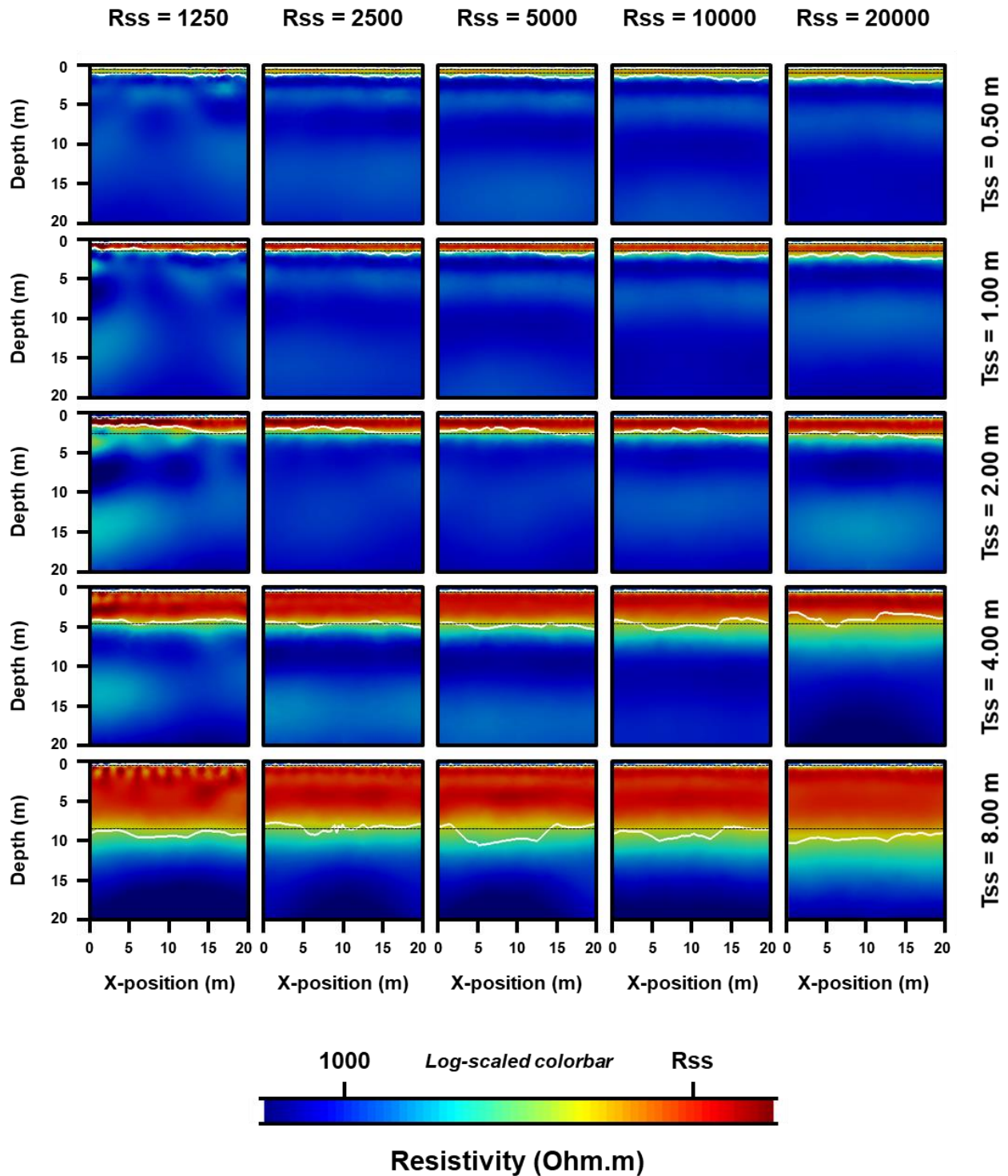


Figure S1: Results of inversion of the synthetic resistivity models (R_{ss} and T_{ss} values stand for the subsolum resistivity and thickness in the model, respectively; ERT-derived and true solum thickness and depth to bedrock interfaces are shown by white and black dashed lines, respectively) using the Wenner-Schlumberger array with an ES of 0.25 m.

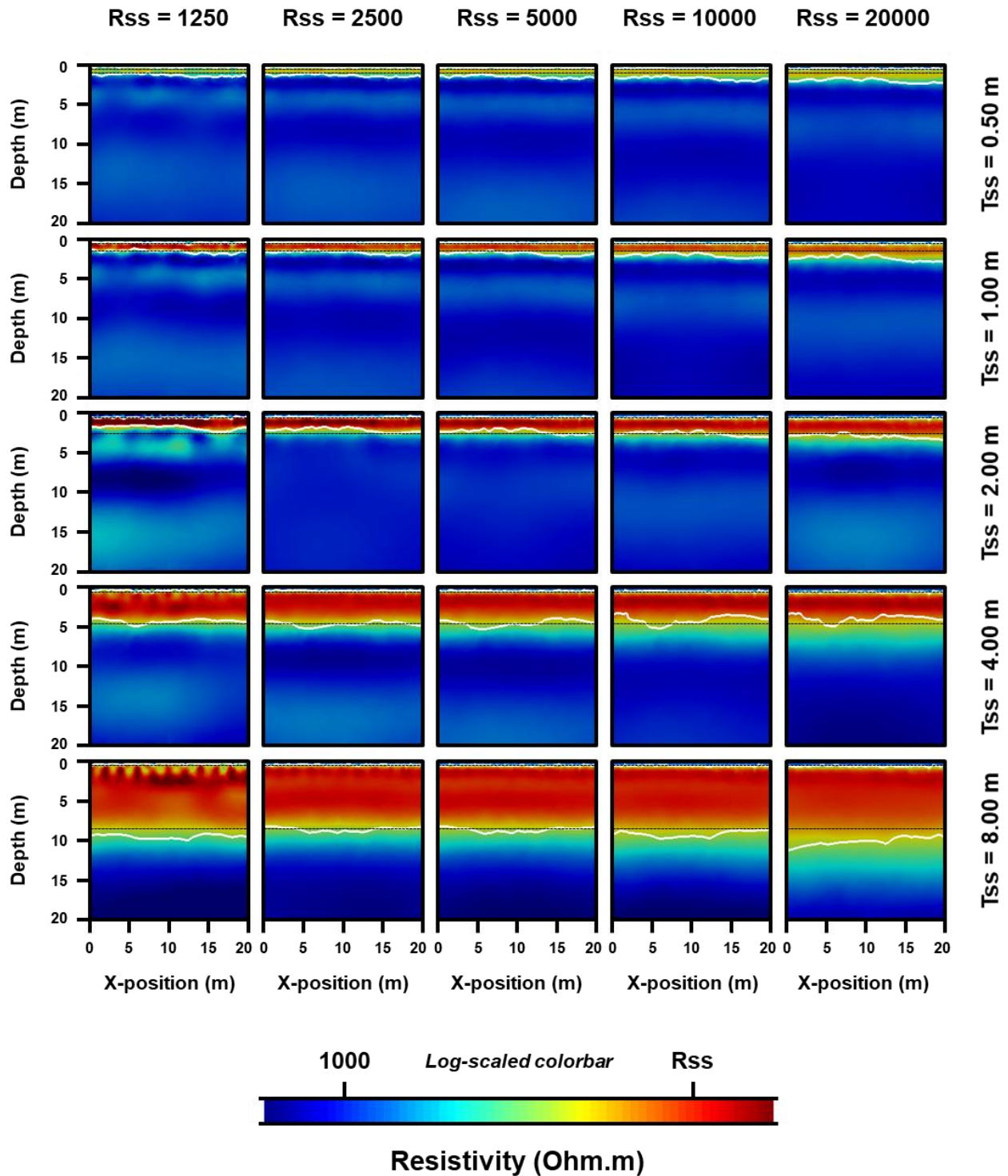


Figure S2: Results of inversion of the synthetic resistivity models (Rss and Tss values stand for the subsolum resistivity and thickness in the model, respectively; ERT-derived and true solum thickness and depth to bedrock interfaces are shown by white and black dashed lines, respectively) using the Wenner-Schlumberger array with an ES of 0.5 m.

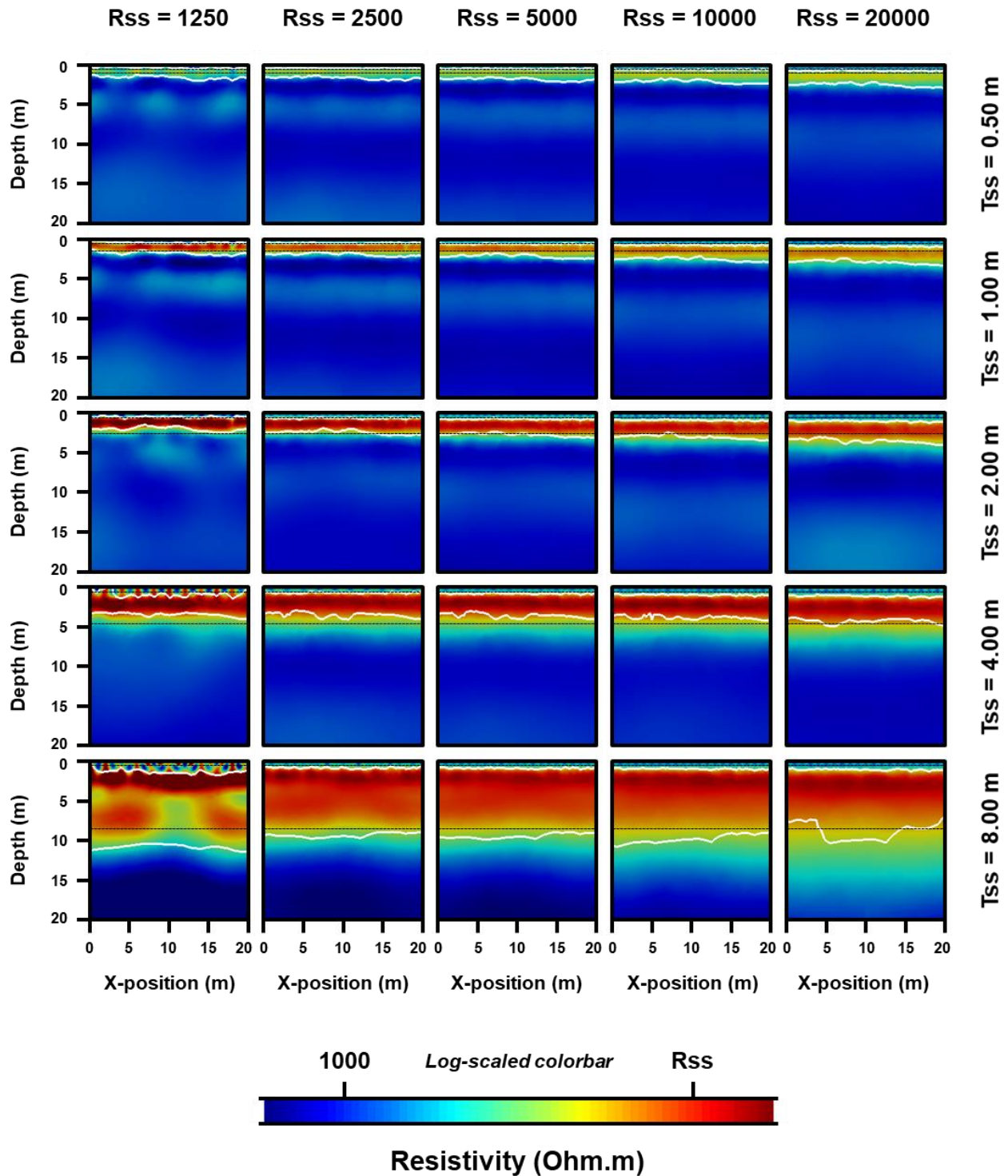


Figure S3: Results of inversion of the synthetic resistivity models (Rss and Tss values stand for the subsolum resistivity and thickness in the model, respectively; ERT-derived and true solum thickness and depth to bedrock interfaces are shown by white and black dashed lines, respectively) using the Wenner-Schlumberger array with an ES of 1 m.

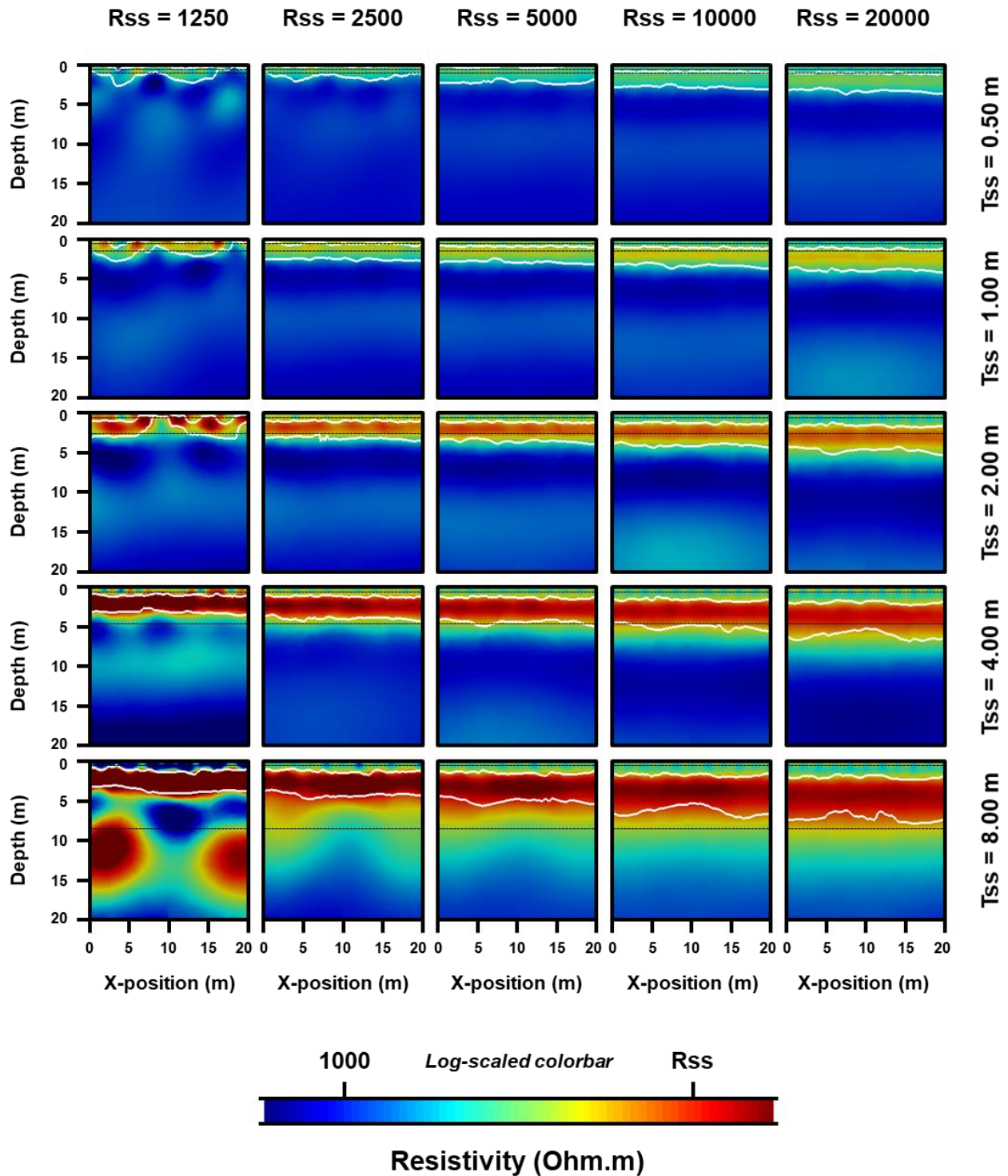


Figure S4: Results of inversion of the synthetic resistivity models (Rss and Tss values stand for the subsolum resistivity and thickness in the model, respectively; ERT-derived and true solum thickness and depth to bedrock interfaces are shown by white and black dashed lines, respectively) using the Wenner-Schlumberger array with an ES of 2 m.

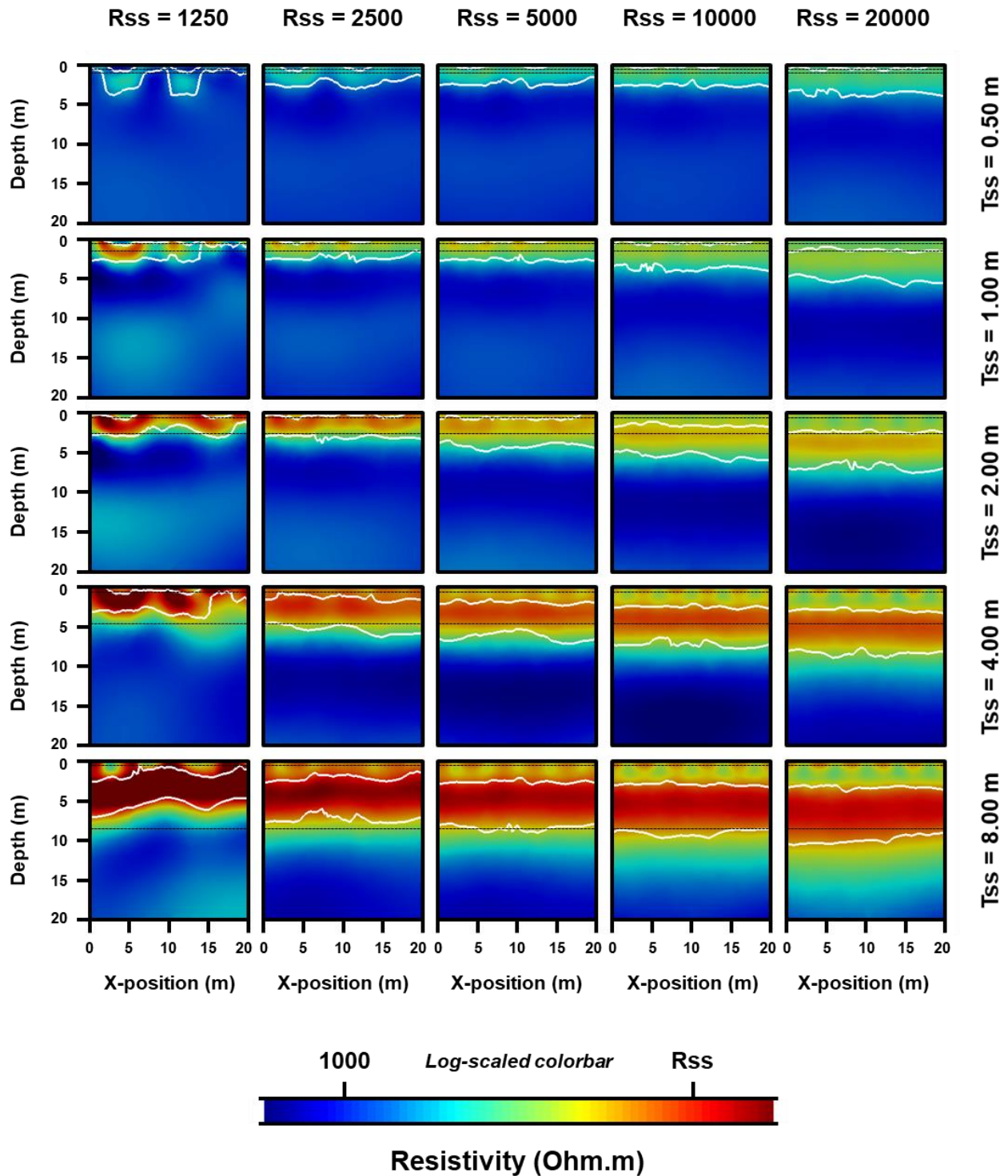


Figure S5: Results of inversion of the synthetic resistivity models (Rss and Tss values stand for the subsolum resistivity and thickness in the model, respectively; ERT-derived and true solum thickness and depth to bedrock interfaces are shown by white and black dashed lines, respectively) using the Wenner-Schlumberger array with an ES of 4 m.

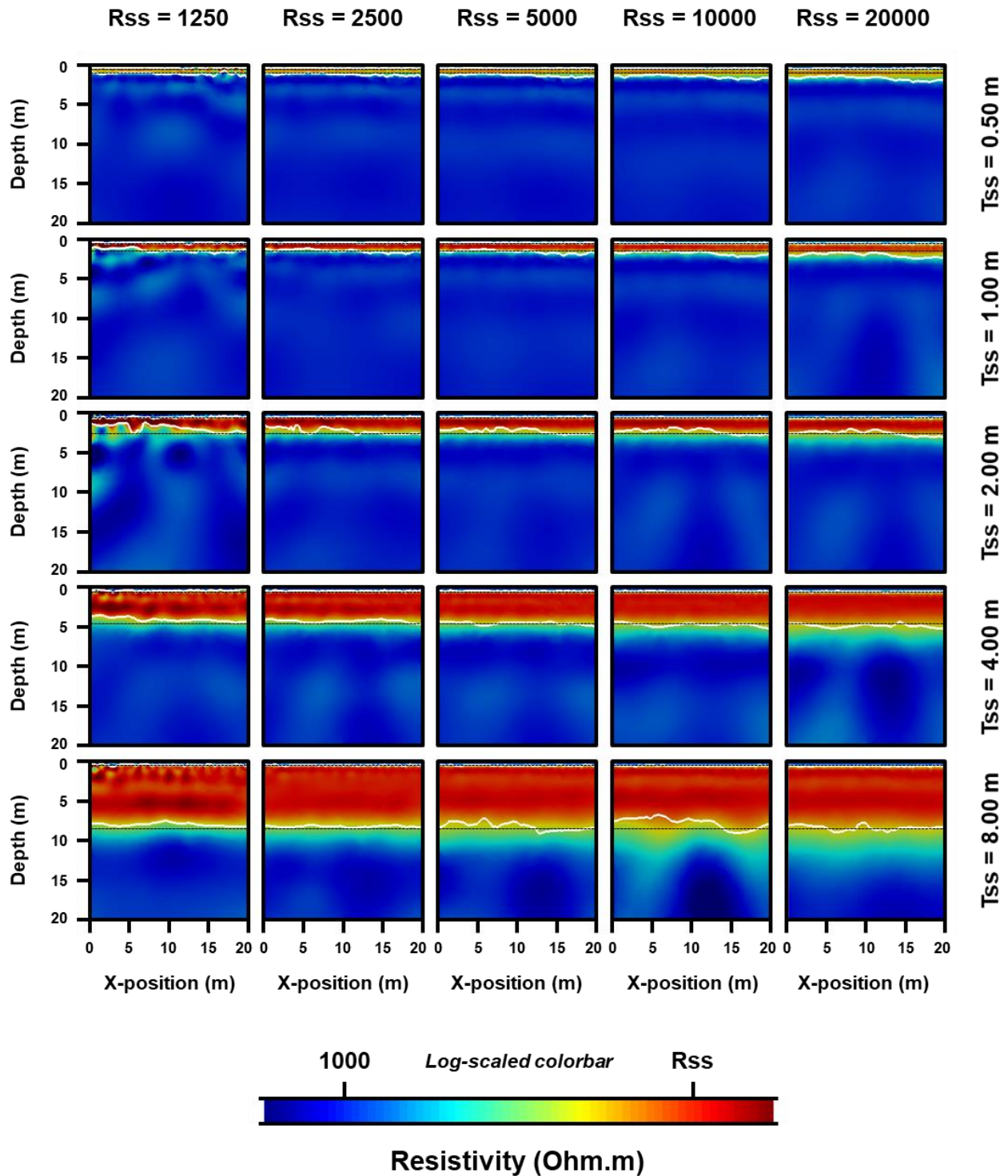


Figure S6: Results of inversion of the synthetic resistivity models (R_{ss} and T_{ss} values stand for the subsolum resistivity and thickness in the model, respectively; ERT-derived and true solum thickness and depth to bedrock interfaces are shown by white and black dashed lines, respectively) using the dipole-dipole array with an ES of 0.25 m.

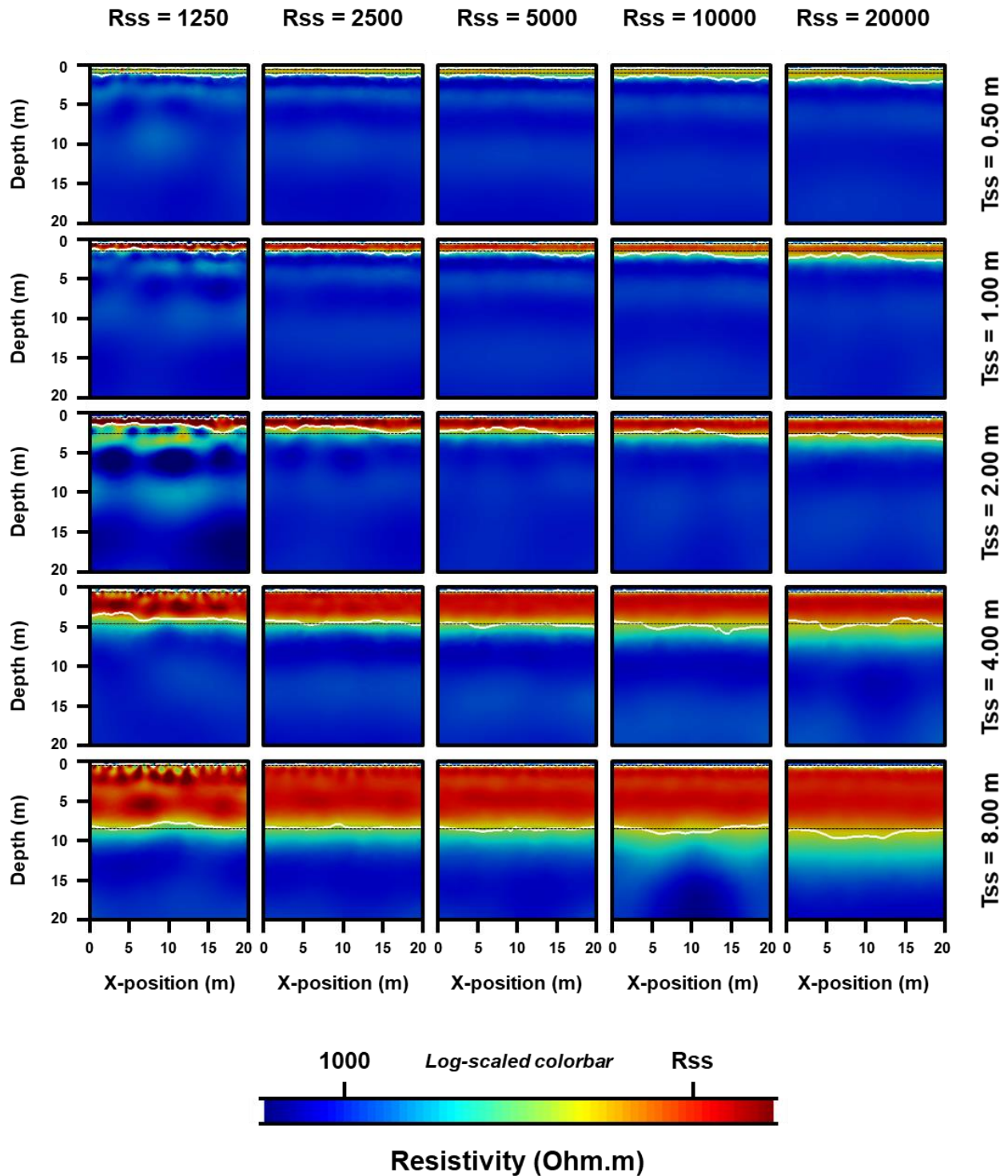


Figure S7: Results of inversion of the synthetic resistivity models (R_{ss} and T_{ss} values stand for the subsolum resistivity and thickness in the model, respectively; ERT-derived and true solum thickness and depth to bedrock interfaces are shown by white and black dashed lines, respectively) using the dipole-dipole array with an ES of 0.5 m.

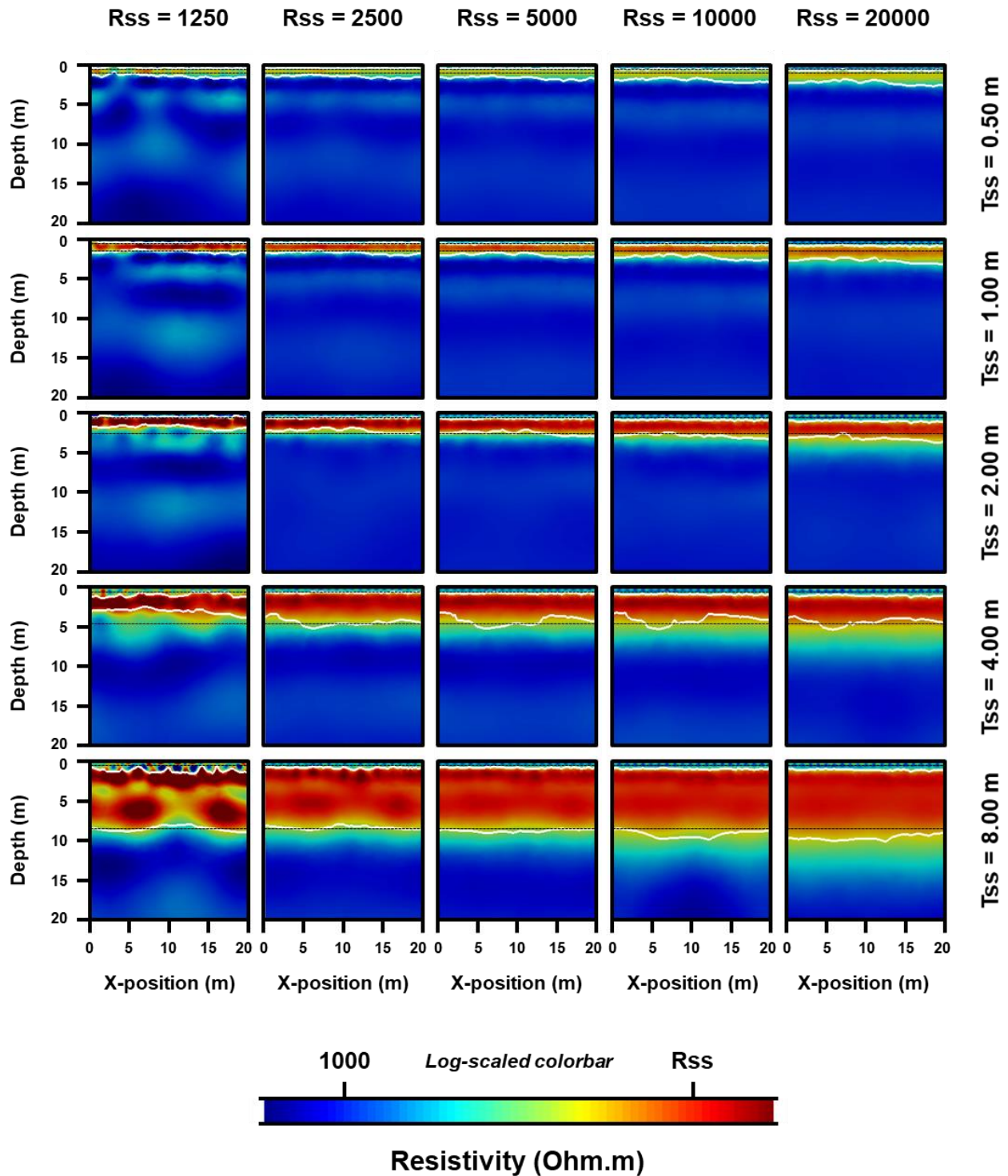


Figure S8: Results of inversion of the synthetic resistivity models (R_{ss} and T_{ss} values stand for the subsolum resistivity and thickness in the model, respectively; ERT-derived and true solum thickness and depth to bedrock interfaces are shown by white and black dashed lines, respectively) using the dipole-dipole array with an ES of 1 m.

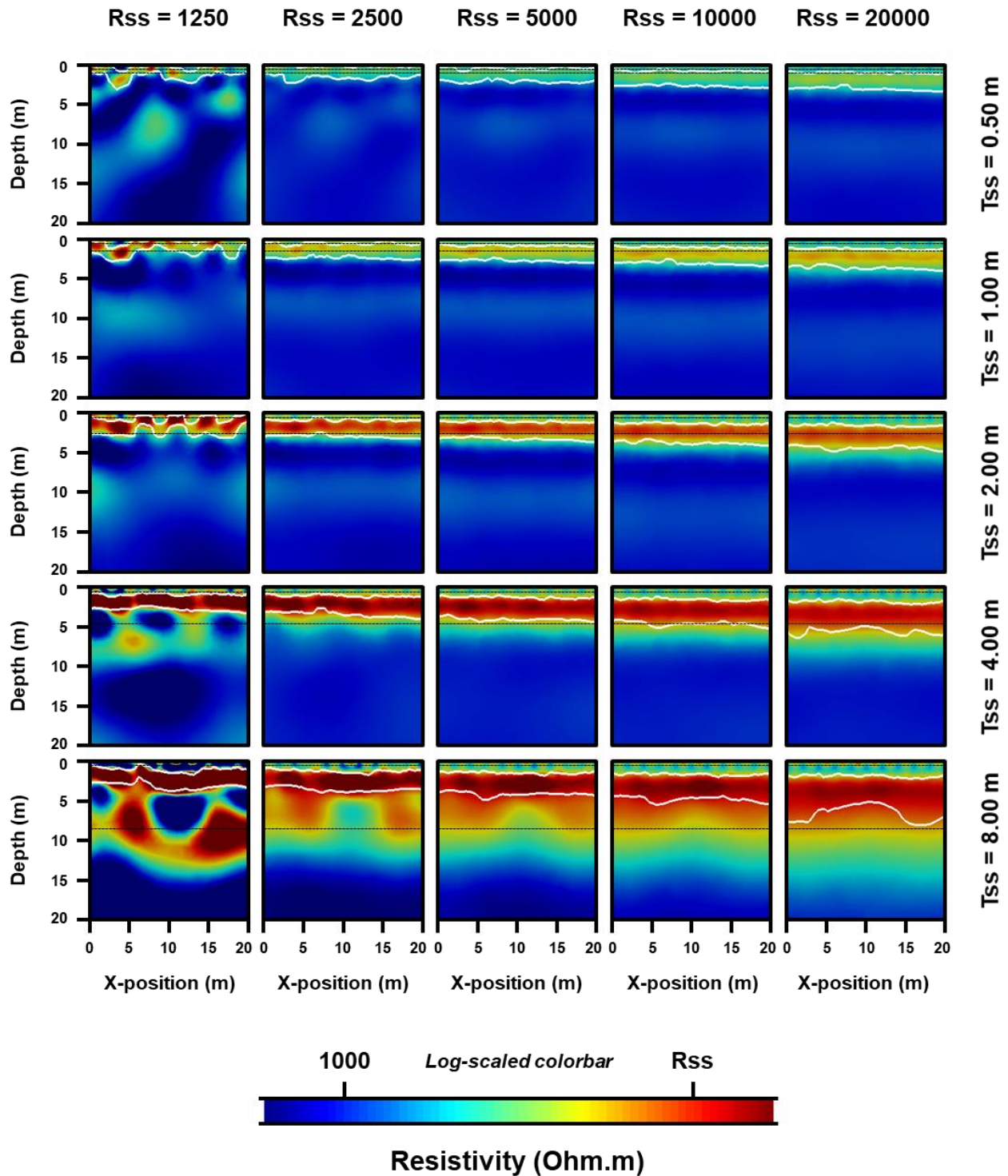


Figure S9: Results of inversion of the synthetic resistivity models (R_{ss} and T_{ss} values stand for the subsolum resistivity and thickness in the model, respectively; ERT-derived and true solum thickness and depth to bedrock interfaces are shown by white and black dashed lines, respectively) using the dipole-dipole array with an ES of 2 m.

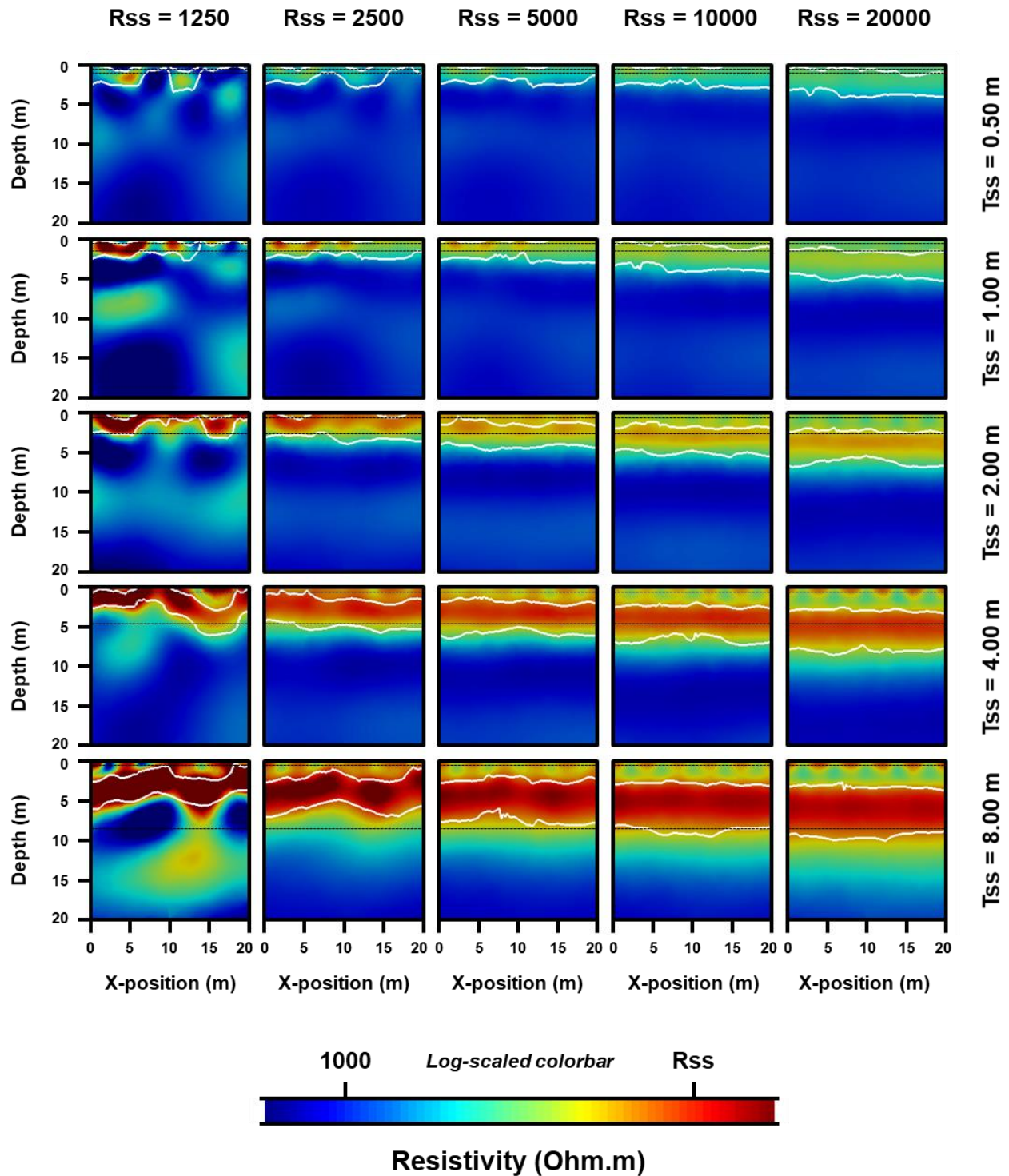


Figure S10: Results of inversion of the synthetic resistivity models (Rss and Tss values stand for the subsolum resistivity and thickness in the model; ERT-derived and true solum thickness and depth to bedrock interfaces are shown by white and black dashed lines, respectively) using the dipole-dipole array with an ES of 4 m.

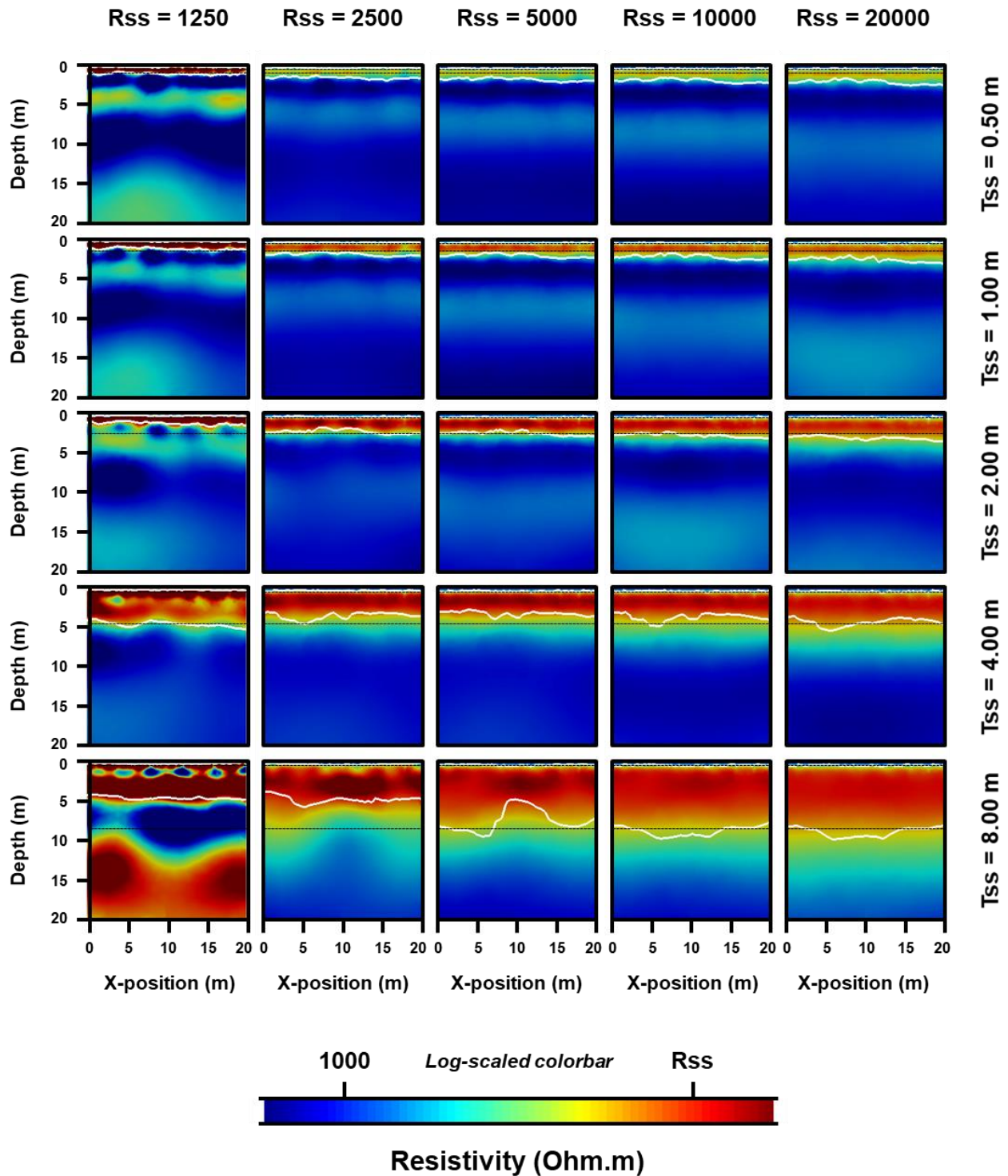


Figure S11: Results of inversion of the synthetic resistivity models (Rss and Tss values stand for the subsolum resistivity and thickness in the model, respectively; ERT-derived and true solum thickness and depth to bedrock true interfaces are shown by white and black dashed lines, respectively) using the Wenner-Schlumberger array with an ES of 2 m and upgraded with the four interpolated levels of surficial apparent resistivity.

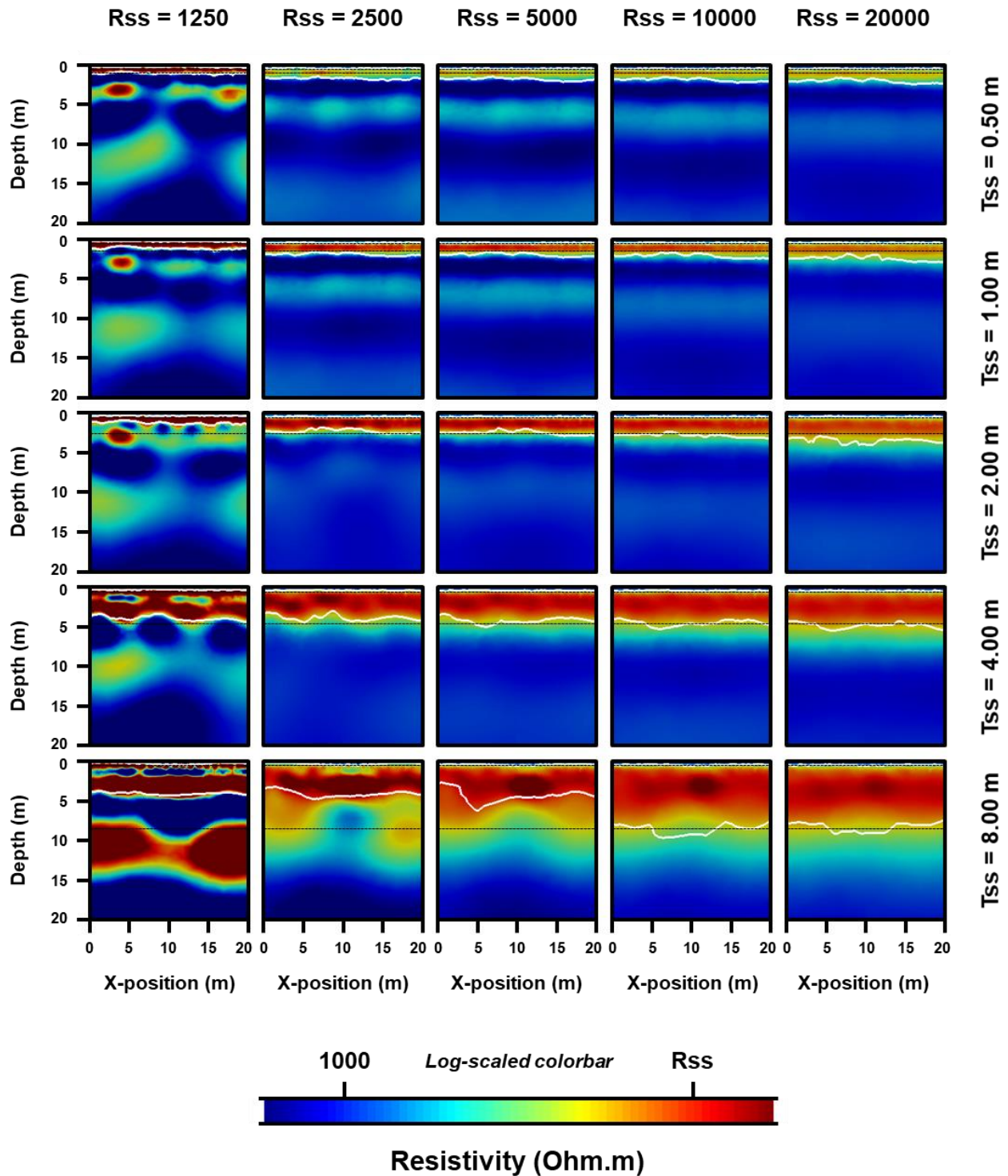


Figure S12: Results of inversion of the synthetic resistivity models (R_{ss} and T_{ss} values stand for the subsolum resistivity and thickness in the model; ERT-derived and true solum thickness and depth to bedrock interfaces are shown by white and black dashed lines, respectively) using the dipole-dipole array with an ES of 2 m and upgraded with the four interpolated levels of surficial apparent resistivity.

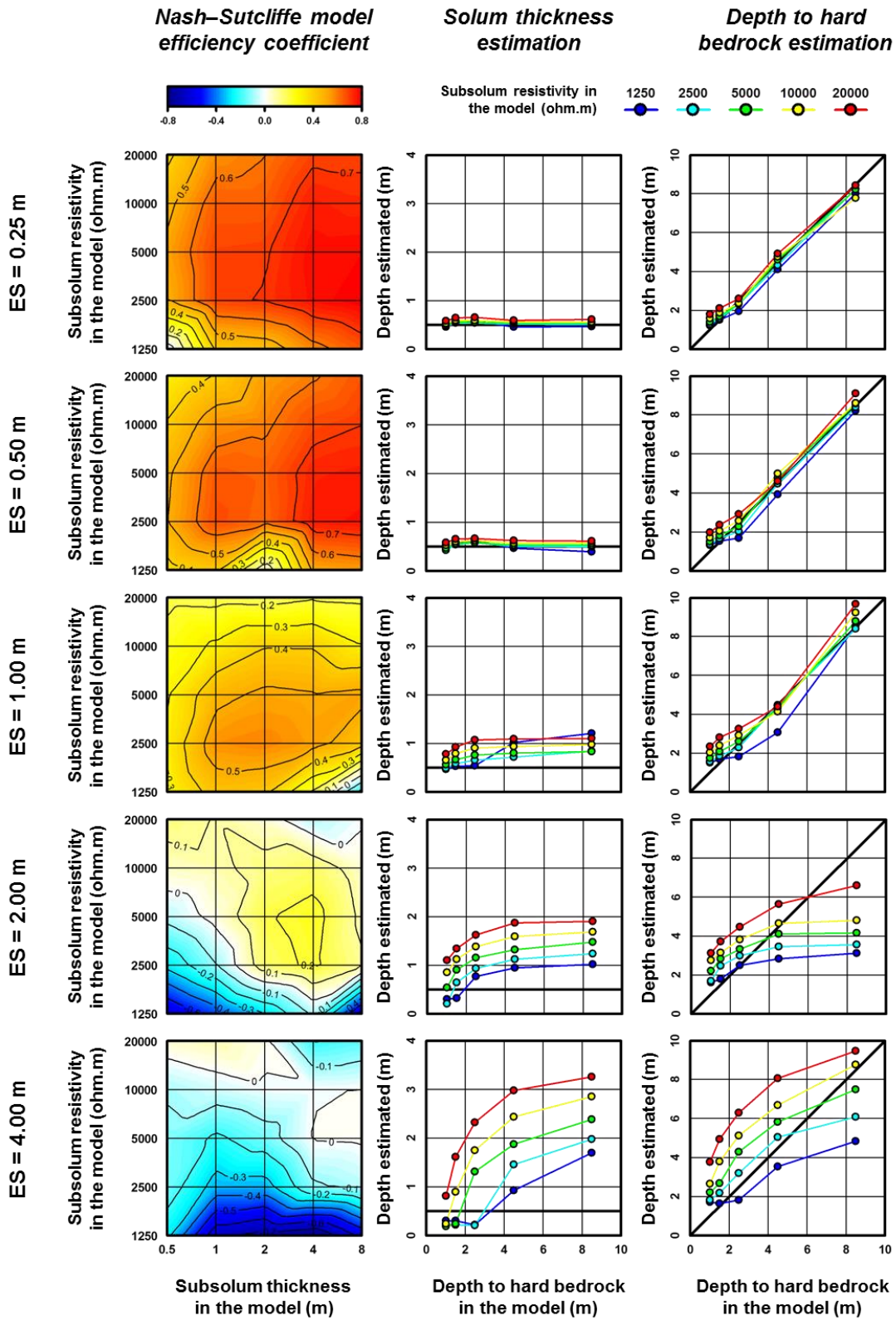


Figure S13: Nash–Sutcliffe model efficiency coefficient and mean interface depths resulting from the inversion of the 25 synthetic apparent resistivity models using the dipole-dipole array with the five different ESs. In plots showing the estimated interface depths, thick black lines indicate the expected values.

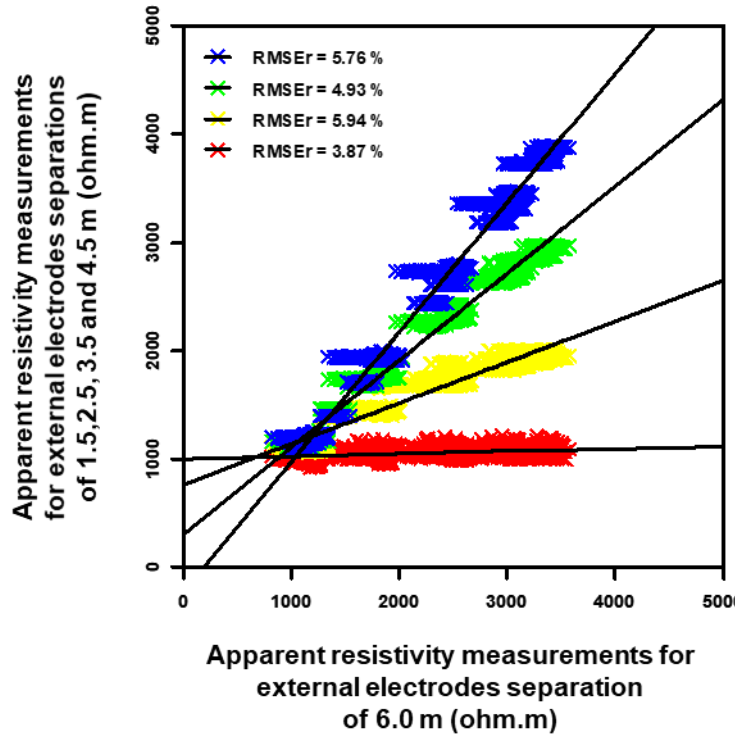


Figure S14: Scatter plots showing the first apparent resistivity level for an ES of 2 m (external electrodes spacing of 6 m) versus the four surficial apparent resistivity levels for an ES of 0.5 m with external electrodes separations of 1.5 (red crosses), 2.5 (yellow crosses), 3.5 (green crosses) and 4.5 m (blue crosses) using the dipole-dipole array for the 25 synthetic resistivity models. The linear regressions correspond to the thick black lines and their accuracy is indicated by the root mean square relative error (RMSEr).

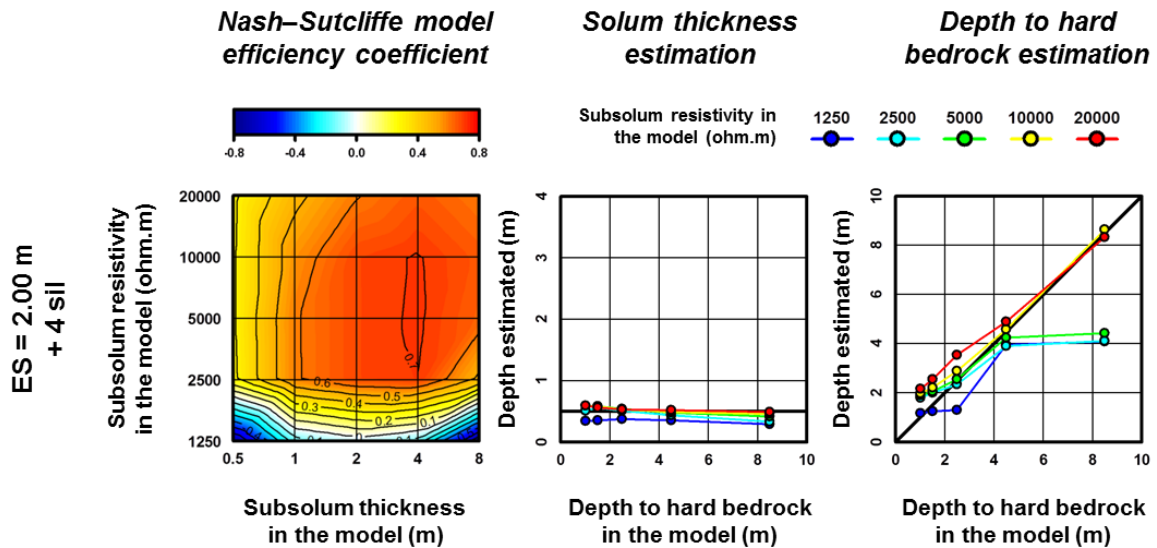


Figure S15: Nash–Sutcliffe model efficiency coefficient and mean interface depths resulting from the inversion of the 25 synthetic apparent resistivity models using the dipole-dipole array with an ES of 2 m and upgraded with the four interpolated levels of surficial apparent resistivity (sil stands for surficial interpolated levels). In plots showing the estimated interface depths, thick black lines indicate the expected values.

Table S1: Nash–Sutcliffe model efficiency coefficient (NSE) and interface depths (avg \pm sd, average \pm standard deviation in m; an italic value specifies that the interface delineation results from the merging of several second derivative zero contours) resulting from the inversion of the 25 synthetic apparent resistivity models (Tss, subsolum thickness in m; Rss, subsolum resistivity in ohm.m) using the dipole-dipole array with the 5 different ESs.

		ES = 0.25 m				ES = 0.50 m				ES = 1.00 m				ES = 2.00 m				ES = 4.00 m																		
Tss	Rss	Solum		Depth to bedrock		Solum		Depth to bedrock		Solum		Depth to bedrock		Solum		Depth to bedrock		Solum		Depth to bedrock		Solum		Depth to bedrock												
		NSE	depth	avg	\pm	sd	NSE	depth	avg	\pm	sd	NSE	depth	avg	\pm	sd	NSE	depth	avg	\pm	sd	NSE	depth	avg	\pm	sd										
0.5	1250	-0.07	0.46	\pm	0.08	1.22	\pm	0.15	0.36	0.44	\pm	0.07	1.35	\pm	0.16	0.28	0.47	\pm	0.08	1.51	\pm	0.19	-0.61	0.31	\pm	0.32	1.62	\pm	0.61	-0.27	0.30	\pm	0.34	1.73	\pm	1.09
0.5	2500	0.50	0.48	\pm	0.05	1.31	\pm	0.13	0.50	0.44	\pm	0.03	1.39	\pm	0.14	0.32	0.49	\pm	0.04	1.58	\pm	0.15	-0.27	0.21	\pm	0.15	1.71	\pm	0.31	-0.14	0.23	\pm	0.27	1.83	\pm	0.82
0.5	5000	0.53	0.51	\pm	0.03	1.42	\pm	0.15	0.48	0.47	\pm	0.04	1.52	\pm	0.15	0.29	0.56	\pm	0.04	1.75	\pm	0.17	-0.07	0.54	\pm	0.17	2.21	\pm	0.18	-0.13	0.19	\pm	0.21	2.21	\pm	0.37
0.5	10000	0.47	0.54	\pm	0.03	1.59	\pm	0.18	0.41	0.53	\pm	0.04	1.72	\pm	0.19	0.24	0.66	\pm	0.05	2.03	\pm	0.21	0.06	0.86	\pm	0.11	2.77	\pm	0.15	-0.09	0.24	\pm	0.19	2.65	\pm	0.31
0.5	20000	0.38	0.59	\pm	0.03	1.81	\pm	0.23	0.30	0.59	\pm	0.04	1.99	\pm	0.24	0.18	0.79	\pm	0.06	2.36	\pm	0.26	0.13	1.11	\pm	0.09	3.14	\pm	0.21	0.05	0.82	\pm	0.34	3.77	\pm	0.38
1	1250	0.42	0.56	\pm	0.06	1.51	\pm	0.23	0.43	0.59	\pm	0.08	1.53	\pm	0.18	0.44	0.53	\pm	0.09	1.69	\pm	0.15	-0.46	0.33	\pm	0.37	1.80	\pm	0.63	-0.67	0.30	\pm	0.27	1.65	\pm	0.80
1	2500	0.68	0.55	\pm	0.03	1.59	\pm	0.18	0.67	0.55	\pm	0.04	1.67	\pm	0.18	0.56	0.58	\pm	0.04	1.85	\pm	0.18	-0.10	0.65	\pm	0.20	2.47	\pm	0.17	-0.34	0.22	\pm	0.18	2.20	\pm	0.34
1	5000	0.68	0.56	\pm	0.03	1.70	\pm	0.20	0.65	0.57	\pm	0.04	1.83	\pm	0.21	0.47	0.67	\pm	0.05	2.09	\pm	0.21	0.03	0.91	\pm	0.10	2.83	\pm	0.16	-0.22	0.24	\pm	0.19	2.68	\pm	0.35
1	10000	0.64	0.60	\pm	0.02	1.88	\pm	0.23	0.56	0.61	\pm	0.04	2.07	\pm	0.24	0.32	0.79	\pm	0.06	2.40	\pm	0.27	0.08	1.12	\pm	0.09	3.17	\pm	0.21	-0.05	0.90	\pm	0.32	3.81	\pm	0.40
1	20000	0.56	0.65	\pm	0.03	2.11	\pm	0.26	0.41	0.66	\pm	0.05	2.38	\pm	0.31	0.17	0.93	\pm	0.07	2.81	\pm	0.26	0.10	1.35	\pm	0.12	3.73	\pm	0.23	0.08	1.61	\pm	0.27	4.95	\pm	0.28
2	1250	0.44	0.59	\pm	0.09	1.97	\pm	0.45	0.01	0.62	\pm	0.10	1.71	\pm	0.34	0.42	0.54	\pm	0.09	1.84	\pm	0.23	-0.31	0.77	\pm	0.41	2.50	\pm	0.61	-0.74	0.22	\pm	0.30	1.84	\pm	0.92
2	2500	0.71	0.55	\pm	0.04	2.32	\pm	0.37	0.63	0.59	\pm	0.06	2.03	\pm	0.31	0.58	0.66	\pm	0.05	2.29	\pm	0.25	0.16	0.94	\pm	0.15	3.01	\pm	0.19	-0.34	0.21	\pm	0.27	3.22	\pm	0.39
2	5000	0.69	0.56	\pm	0.04	2.34	\pm	0.28	0.63	0.59	\pm	0.05	2.31	\pm	0.28	0.52	0.76	\pm	0.06	2.61	\pm	0.25	0.19	1.16	\pm	0.09	3.34	\pm	0.19	-0.15	1.32	\pm	0.30	4.30	\pm	0.25
2	10000	0.64	0.59	\pm	0.04	2.38	\pm	0.30	0.58	0.63	\pm	0.05	2.59	\pm	0.27	0.39	0.91	\pm	0.07	2.91	\pm	0.23	0.13	1.39	\pm	0.11	3.83	\pm	0.21	-0.01	1.75	\pm	0.26	5.13	\pm	0.28
2	20000	0.60	0.66	\pm	0.04	2.60	\pm	0.30	0.53	0.67	\pm	0.06	2.93	\pm	0.23	0.16	1.08	\pm	0.08	3.25	\pm	0.27	0.04	1.63	\pm	0.14	4.47	\pm	0.23	0.02	2.32	\pm	0.18	6.31	\pm	0.47
4	1250	0.57	0.47	\pm	0.09	4.11	\pm	0.25	0.51	0.47	\pm	0.15	3.92	\pm	0.33	0.19	1.02	\pm	0.24	3.09	\pm	0.34	-0.08	0.95	\pm	0.14	2.85	\pm	0.23	-0.93	0.93	\pm	0.95	3.55	\pm	1.52
4	2500	0.77	0.53	\pm	0.04	4.32	\pm	0.16	0.75	0.51	\pm	0.06	4.49	\pm	0.16	0.53	0.72	\pm	0.07	4.49	\pm	0.43	0.22	1.13	\pm	0.14	3.47	\pm	0.37	-0.11	1.46	\pm	0.50	5.06	\pm	0.41
4	5000	0.77	0.54	\pm	0.04	4.61	\pm	0.16	0.74	0.54	\pm	0.05	4.78	\pm	0.17	0.51	0.81	\pm	0.07	4.31	\pm	0.59	0.24	1.33	\pm	0.14	4.12	\pm	0.20	0.01	1.88	\pm	0.29	5.84	\pm	0.39
4	10000	0.75	0.57	\pm	0.04	4.78	\pm	0.21	0.67	0.57	\pm	0.05	5.01	\pm	0.35	0.39	0.94	\pm	0.07	4.14	\pm	0.60	0.16	1.59	\pm	0.15	4.67	\pm	0.28	-0.01	2.43	\pm	0.18	6.70	\pm	0.48
4	20000	0.68	0.60	\pm	0.04	4.92	\pm	0.21	0.59	0.63	\pm	0.05	4.62	\pm	0.38	0.19	1.10	\pm	0.08	4.40	\pm	0.44	-0.08	1.88	\pm	0.18	5.64	\pm	0.41	-0.21	2.97	\pm	0.17	8.06	\pm	0.25
8	1250	0.65	0.47	\pm	0.08	8.01	\pm	0.19	0.54	0.40	\pm	0.14	8.23	\pm	0.28	-0.24	1.21	\pm	0.26	8.54	\pm	0.30	-0.65	1.03	\pm	0.32	3.13	\pm	0.42	-0.58	1.70	\pm	0.67	4.85	\pm	0.68
8	2500	0.80	0.52	\pm	0.04	8.25	\pm	0.10	0.77	0.50	\pm	0.05	8.39	\pm	0.12	0.44	0.85	\pm	0.10	8.40	\pm	0.19	0.11	1.25	\pm	0.19	3.57	\pm	0.29	-0.08	1.98	\pm	0.55	6.08	\pm	0.67
8	5000	0.78	0.54	\pm	0.04	8.23	\pm	0.48	0.75	0.54	\pm	0.05	8.58	\pm	0.14	0.52	0.84	\pm	0.07	8.79	\pm	0.16	0.08	1.48	\pm	0.13	4.16	\pm	0.28	0.01	2.38	\pm	0.33	7.50	\pm	0.56
8	10000	0.73	0.57	\pm	0.04	7.77	\pm	0.68	0.70	0.58	\pm	0.05	8.61	\pm	0.36	0.30	0.98	\pm	0.06	9.22	\pm	0.42	0.05	1.69	\pm	0.13	4.82	\pm	0.34	0.00	2.85	\pm	0.17	8.78	\pm	0.44
8	20000	0.69	0.61	\pm	0.04	8.42	\pm	0.30	0.66	0.62	\pm	0.05	9.12	\pm	0.40	0.18	1.10	\pm	0.08	9.66	\pm	0.31	-0.01	1.90	\pm	0.18	6.61	\pm	1.04	-0.17	3.25	\pm	0.20	9.48	\pm	0.35

Table S2: Nash–Sutcliffe model efficiency coefficient (NSE) and interface depths (avg \pm sd, average \pm standard deviation in m; an italic value specifies that the interface delineation has gone through the merging of several second derivative zero contours) resulting from the inversion of the 25 synthetic apparent resistivity models (Tss, subsolum thickness in m; Rss, subsolum resistivity in ohm.m) using the dipole-dipole array with the ES of 2 m upgraded with the four interpolated levels of surficial apparent resistivity (sil stands for surficial interpolated levels).

$$\text{ES} = 2.00 \text{ m} + 4\text{sil}$$

Tss	Rss	Solum			Depth to bedrock		
		NSE	depth	avg \pm sd	avg \pm sd	bedrock	
0.5	1250	-0.74	0.35 \pm 0.05	1.18 \pm 0.10			
0.5	2500	0.28	0.51 \pm 0.09	1.82 \pm 0.12			
0.5	5000	0.29	0.60 \pm 0.05	1.91 \pm 0.17			
0.5	10000	0.29	0.59 \pm 0.04	1.98 \pm 0.20			
0.5	20000	0.28	0.60 \pm 0.05	2.16 \pm 0.24			
1	1250	-0.15	0.36 \pm 0.04	1.26 \pm 0.14			
1	2500	0.59	0.57 \pm 0.07	2.01 \pm 0.16			
1	5000	0.59	0.59 \pm 0.05	2.07 \pm 0.20			
1	10000	0.56	0.58 \pm 0.05	2.21 \pm 0.25			
1	20000	0.47	0.57 \pm 0.05	2.57 \pm 0.29			
2	1250	-0.05	0.38 \pm 0.04	1.31 \pm 0.17			
2	2500	0.68	0.52 \pm 0.07	2.35 \pm 0.25			
2	5000	0.68	0.54 \pm 0.06	2.55 \pm 0.26			
2	10000	0.68	0.53 \pm 0.05	2.89 \pm 0.21			
2	20000	0.59	0.54 \pm 0.05	3.53 \pm 0.31			
4	1250	-0.14	0.36 \pm 0.05	3.96 \pm 0.29			
4	2500	0.70	0.44 \pm 0.05	3.90 \pm 0.36			
4	5000	0.71	0.48 \pm 0.05	4.25 \pm 0.38			
4	10000	0.70	0.49 \pm 0.06	4.57 \pm 0.37			
4	20000	0.65	0.52 \pm 0.05	4.90 \pm 0.35			
8	1250	-1.56	0.29 \pm 0.11	4.09 \pm 0.15			
8	2500	0.48	0.34 \pm 0.11	4.13 \pm 0.41			
8	5000	0.63	0.43 \pm 0.08	4.42 \pm 0.84			
8	10000	0.65	0.47 \pm 0.06	8.64 \pm 0.63			
8	20000	0.60	0.50 \pm 0.06	8.33 \pm 0.55			